RESEARCH ARTICLE | JANUARY 07 2025

Stem cell mechanoadaptation. II. Microtubule stabilization and substrate compliance effects on cytoskeletal remodeling

Vina D. L. Putra ; Kristopher A. Kilian ; Melissa L. Knothe Tate

APL Bioeng. 9, 016103 (2025)
https://doi.org/10.1063/5.0231287

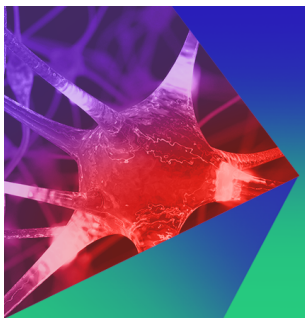

Stem cell mechanoadaptation. II. Microtubule stabilization and substrate compliance effects on cytoskeletal remodeling

Cite as: APL Bioeng. **9**, 016103 (2025); doi: 10.1063/5.0231287
Submitted: 30 July 2024 · Accepted: 1 December 2024 ·
Published Online: 7 January 2025

Vina D. L. Putra,[1] Kristopher A. Kilian,[1,a)] and Melissa L. Knothe Tate[2,a)]

AFFILIATIONS

[1]School of Chemistry and School of Materials Science & Engineering, University of New South Wales, Sydney, NSW, Australia
[2]Blue Mountains World Interdisciplinary Innovation Institute (bmwi^3) Australia

[a)]**Authors to whom correspondence should be addressed:** proftate.bmwi3@gmail.com and k.kilian@unsw.edu.au

ABSTRACT

Stem cells adapt to their local mechanical environment by rearranging their cytoskeleton, which underpins the evolution of their shape and fate as well as the emergence of tissue structure and function. Here, in the second part of a two-part experimental series, we aimed to elucidate spatiotemporal cytoskeletal remodeling and resulting changes in morphology and mechanical properties of cells and their nuclei. Akin to mechanical testing of the most basic living and adapting unit of life, i.e., the cell, *in situ* in model tissue templates, we probed native and microtubule-stabilized (via Paclitaxel, PAX, exposure) stem cells' cytoskeletal adaptation capacity on substrates of increasing compliance (exerting local tension on cells) and with increased target seeding densities (exerting local compression on cells). On 10 and 100 kPa gels, cells seeded at 5000 cells/cm^2 and cells proliferated to 15 000 cells/cm^2 exhibited bulk moduli that nearly matched those of their respective substrates; hence, they exhibited a greater increase in Young's Modulus after microtubule stabilization than cells cultured on glass. Culture on compliant substrates also reduced microtubule-stabilized cells' F-actin, and microtubule concentration increases compared to cells seeded on glass. On gels, F-actin alignment decreased as more randomly oriented, short actin crosslinks were observed, representing emergent adaptation to the compliant substrate, mediated through myosin II contractility. We conclude that stem cell adaptation to compliant substrates facilitates the accommodation of larger loads from the PAX-stabilized polymerizing microtubule, which, in turn, exerts a larger effect in determining cells' capacity to stiffen and remodel the cytoskeleton. Taken as a whole, these studies establish correlations between cytoskeleton and physical and mechanical parameters of stem cells. Hence, the studies progress our understanding of the dynamic cytoskeleton as well as shape changes in cells and their nuclei, culminating in emergent tissue development and healing.

INTRODUCTION

Across the time and length scales of tissue development, stem cells adapt to the dynamic biomechanical and biophysical cues that determine the mechanical properties of their niche or tissue habitat.[1,2] Over time, stem cells proliferate and grow, forming multicellular constructs with higher order architectures enabling more specialized functions. This process is exemplified *in situ* and *in vivo* by the process of tissue template (*Anlage*) development, e.g., formation of the condensing mesenchyme as the initial step in musculoskeletal development.[2,3]

Previously published work demonstrated the capacity of physiological stresses, *i.e.*, intrinsic to growth, development, and maintenance of tissues,[4,5,7,8] to modulate cell and nuclear morphometries,[9,11] which tie closely to evolving cytoskeletal architectures,[6,11] e.g., flattening of the nucleus via formation of an actin cap over and around the nucleus.[10] Such force-mediated modulation of cell and nuclear morphology has been shown to alter baseline gene expression of early mesenchymal condensation markers characteristic of emergent skeletogenesis as well as the expression of F-actin and tubulin filaments.[6,11] Following on our studies probing mesenchymal stem cell (MSC) mechanoadaptation using exogenous modulators of cytoskeletal remodeling and local compression induced by seeding at increasing densities [see (Part I)],[11] here (Part II), we examine effects of substrate compliance (or respective stiffness) on cell and nuclear morphology, cytoskeletal remodeling, and emergent lineage determination.

We modulated the cells' capacity to regulate stiffness and generate forces via exogenous exposure to Paclitaxel (PAX, which inhibits

microtubule depolymerization), using methods described in the first part of these studies [Part I].[11] We hypothesized that the compliance of the substrate, together with local compression experienced by cells, and exposure to PAX, individually and together, influence the spatio-temporal remodeling of the cytoskeleton. To that end, we measured the spatial distribution of the cytoskeleton; changes in cell volume, shape, and stiffness; and nucleus volume and shape over time periods relevant for early developmental processes (24, 48, and 72 h). By quantifying the time and PAX concentration-dependent changes in cell viability, proliferation, and cytoskeletal reorganization, we elucidated the cells' mechanoadaptation capacity in contexts, mimicking those that occur during early stages of tissue development.

RESULTS

Substrate compliance modulates the cell volume increases and shape changes mediated by microtubule stabilization

To elucidate mechanoadaptation, as cells are subjected to as well as sense and counteract boundary forces, e.g., from the underlying substrate and/or surrounding cells, we introduced a range of polyacrylamide hydrogel substrates more compliant than glass, from stiffest gels (100 and 10 kPa gels) to softest gels as compliant as cells themselves (1 kPa gels). To test the hypothesis that changes in stiffness at cell boundaries (substrate compliance) as well as intrinsic cell stiffness and size modulate force balances driving mechanoadaptation, we measured cell volume and corresponding actin filament alignment and cell stiffness, in association with culture on substrates of increasing compliance (decreasing resistance at cell boundaries) and PAX exposure (inhibiting tubulin depolymerization and increasing cell stiffness and volume).

Effect of more compliant substrates on cell morphology

Substrate compliance exerts a profound influence on the local environment and subsequent adaptation of cell behavior (structure–function). Cell spreading was similar on the 10 and 100 kPa gel substrates; however, on the softest 1 kPa gel, most cells showed reduced spreading and exhibited comparatively rounder morphology [Fig. 1(a)]. Cells seeded on the stiffest, *i.e.,* glass, substrate showed greater changes in morphology across observation timepoints than those seeded on more compliant gel substrates, where significant and grossly observable changes were observed first at the 72 h timepoint [Fig. 1(b)]. The cell volume increase associated with 100 nM PAX exposure shows comparable magnitude across the gel stiffnesses. However, with lower PAX concentrations on softer gels, cell volume remained small. As a result, cell shape measures (SA/V) were also generally smaller, indicative of rounder cells, for cells seeded on gels compared to those seeded on glass [Fig. 1(c)].

Subtle changes in cell morphology [Fig. S1(a)], volume [Fig. S1(b)], shape [Fig. S1(c)], and spreading were observed as cells were adapting to softer substrates than to glass at 24 h, although significant changes observed only in cells seeded on glass substrates. At 48 h [Fig. S1(d)], PAX concentration-dependent cell volume increases were observed with increasing substrate stiffness [Fig. S1(e)], as was cell flattening [Fig. S1(f)].

PAX-induced changes in cell volume and actin alignment regulate stem cell rigidity sensing that is enhanced in cells proliferating to high density

Effect of more compliant substrates on cytoskeleton filament concentration and spatial distribution

To study how cell volume adaptation on soft substrates translates to changes in cytoskeletal structure [Fig. 2(a)], we measured the spatial

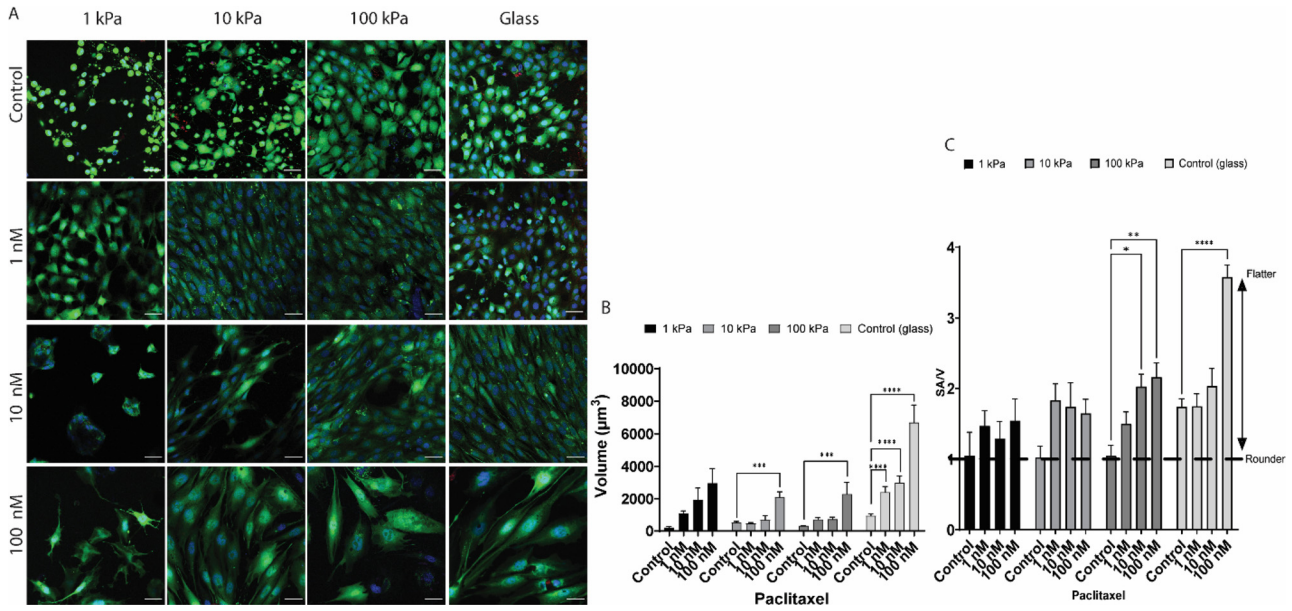

FIG. 1. Compliant substrates modulate PAX concentration-dependent cell volume increases. (a) After 72 h of PAX exposure, cells seeded on compliant gel substrates (scale bar 50 μm) show smaller volume and smaller increases in volume with increasing PAX concentration (b). With increasing substrate stiffness, cells exhibit average larger SA/V and the largest increase on glass (c) than those seeded gels due to their smaller volume. Asterisk(s) indicate significant difference at $^{****}p < 0.001$, $^{***}p < 0.01$, $^{**}p < 0.01$, and $^{*}p < 0.05$. Two-way ANOVA with Tukey's multiple comparison test.

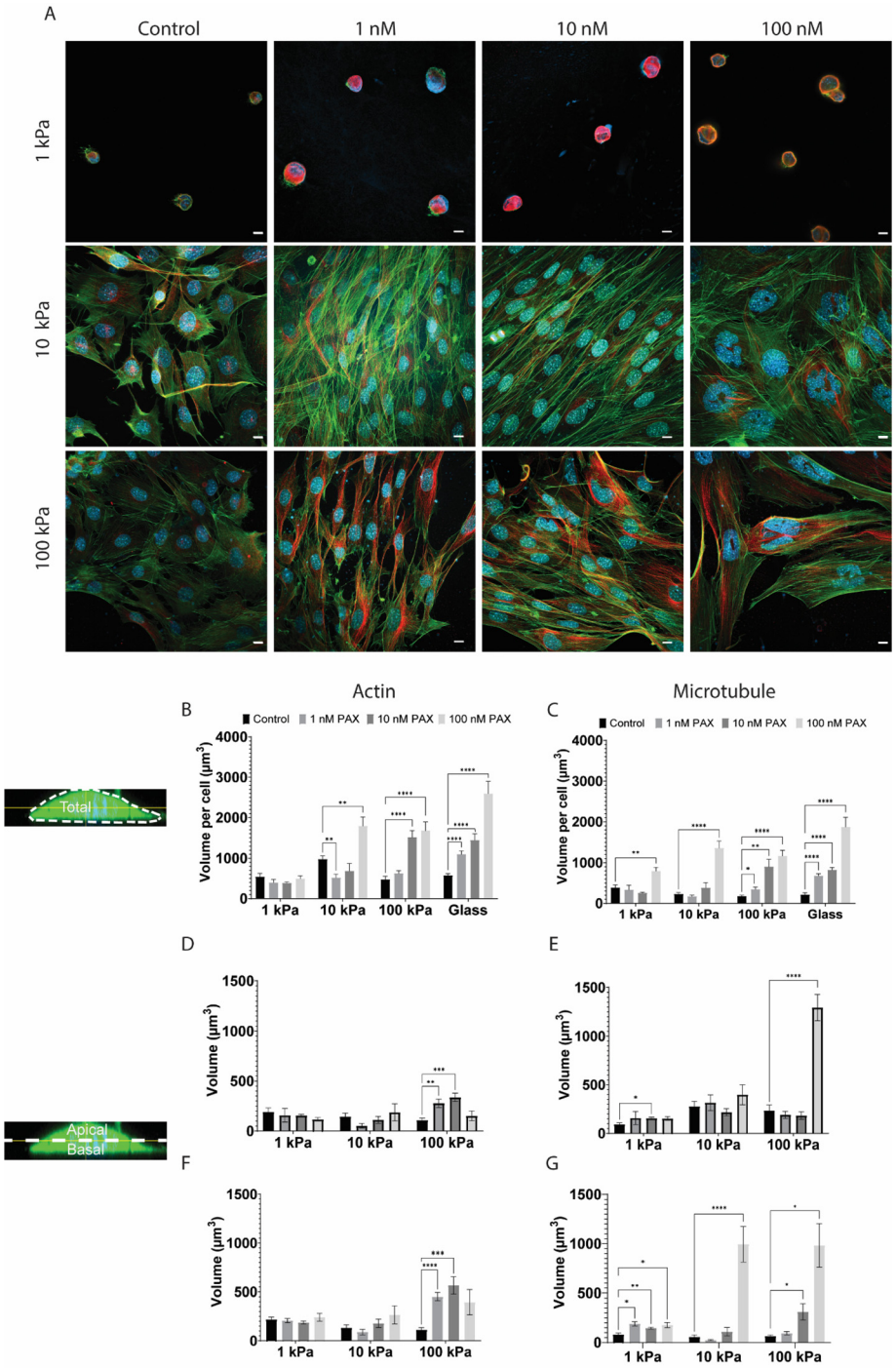

FIG. 2. Changes in cytoskeletal spatial distribution provide a means for cells to adapt to substrate stiffness. (a) Culture on compliant substrates modulates cytoskeletal structure (scale bar = 10 μm) upon stabilization of microtubule with PAX and the PAX concentration-dependent increase in (b) F-actin and (c) microtubule concentration per cell, apart from the 1 and 10 nM PAX on the softest (1 and 10 kPa) gel substrates. Segmenting the cell into apical and basal regions revealed fewer PAX-concentration dependent differences in respective volumes of F-actin (d) and (f) or microtubule (e) and (g). Taken as a whole, larger and more significant differences were observed in the amount of microtubule in the basal regions of the PAX exposed cells compared to controls. Measurement of the actin and microtubule concentration per cell was carried out in three repeats of immunofluorescence labeling followed by imaging. Each repeat included 10–15 cells. Asterisk(s) indicate significant difference at $^{****}p < 0.001$, $^{***}p < 0.01$, $^{**}p < 0.01$, and $^{*}p < 0.05$. Two-way ANOVA with Tukey's multiple comparison test.

distribution and alignment of cytoskeleton in cells exposed to increasing concentrations of PAX and cultured on the 1, 10, and 100 kPa gels after 72 h. Concentration-dependent cytoskeletal remodeling was observable as an increase in the amount both actin [Fig. 2(b)] and microtubule [Fig. 2(c)] per cell with increasing concentration of PAX, for all groups, **except** cells exposed to 1 and 10 nM (lower concentrations) PAX and seeded on softest gel substrates (1 and 10 kPa). When we segmented actin and microtubules into the apical [Figs. 2(d) and 2(e)] and basal [Figs. 2(f) and 2(g)] regions of cells exposed to PAX and cultured on gel substrates, concentration-dependent differences

nearly disappeared across all substrate compliances. Hence, early (over 72 h in culture) mechanoadaptation of stem cells to substrates of different stiffnesses and in conjunction with PAX exposure appears to involve bulk increases in cytoskeletal proteins F-actin and tubulin without overt evidence of emergent cytoskeletal polarity at 72 h.

Effect of more compliant substrates on F-actin alignment

Grossly visible changes in F-actin alignment occurred with both increasing substrate stiffness, from 1 to 100 kPa, and with exposure to increasing concentrations of PAX, except in cells seeded on the softest (1 kPa) gel substrates [Fig. 3(a)]. In fact, cells cultured on 1 kPa gel and exposed to PAX showed less F-actin alignment than control cells not exposed to PAX [Fig. 3(b)]. On 10 and 100 kPa substrates, F-actin alignment of cells exposed to 1 nM PAX was lower than that of unexposed control cells [Figs. 3(c) and 3(d)]; in contrast, on the same substrates, F-actin alignment of cells exposed to higher concentrations of PAX (10 and 100 nM) demonstrated, respectively, higher actin alignment than that of unexposed control cells [Figs. 3(c) and 3(d)], with respective differences slightly higher on the 100 kPa compared to the 10 kPa gel substrate. Actin alignment in cells cultured on 10 [Fig. 3(c)] and 100 kPa [Fig. 3(d)] gels showed similar alignment to cells cultured on glass [Part I, Fig. 2(a)]. Differences in the apical-basal alignment of the cytoskeleton were not distinguishable between PAX-exposed groups across the 1 [Fig. 3(e)], 10 [Fig. 3(f)], and 100 [Fig. 3(g)] kPa gel substrates. Hence, it appears that F-actin alignment is more strongly associated with mechanoadaptation to increasing stiffness substrates, which are significantly **stiffer than the cells themselves**, i.e., 10 and 100 kPa gel substrates and glass, and is shifted slightly higher with inhibition of depolymerization via exposure to PAX at 10 and 100 nM.

Effect of more compliant substrates on cells' mechanical properties

Cells do not possess a pre-defined stiffness. Furthermore, increasing intrinsic cell stiffness and/or cytoskeleton-generated forces may drive cell mechanoadaptation over the 72 h observation period to balance forces at the boundary of the cell to its local environment. Hence, we next probed the stiffness (via AFM) of cells cultured on gel substrates and correlated changes in stiffness to actin alignment (as described earlier). Compared to control cells seeded on glass, stiffness of cells on compliant substrates more closely matched the stiffness of their underlying substrate, and this adaptive cell stiffening increased with PAX exposure. Considering control cells cultured on substrates of increasing stiffness, on 10 kPa [Fig. 4(a)] and 100 kPa gels [Fig. 4(b)], control cells showed a mean respective Young's Modulus of 8.08 and 15.25 kPa; previously (Part I), we found that control cells on glass substrates ($4 \pm 2 \times 10^6$ kPa) exhibited a mean Young's Modulus of 3.3 kPa. PAX-exposed cells exhibited higher stiffness [Fig. 4(c)], both on 10 and 100 kPa gel substrates where they exhibited higher respective mean Young's Moduli of 10.9 and 23.08 kPa and on glass where they exhibited a mean Young's Modulus of 6.4 kPa.

To probe mechanistically how this contrasting change in Young's Modulus after PAX treatment could be modulated by underlying substrate stiffness, we harvested the cells after culture on gel substrates and exposure to PAX for 48 h and measured the stiffness of the resulting suspended cells using deformability cytometry. The difference (increase) in Young's Modulus between control and PAX-treated, suspended cells after culture on 10 kPa gel and 100 kPa gel was as significant as the respective difference in Young's Modulus of suspended cells cultured on glass [Fig. 4(d)]. The larger, irregular morphology of PAX-treated cells seeded on the gel could still be observed when they were flushed through the channel; however, they exhibited a smaller area [Fig. S2(a)] and volume [Fig. S2(b)] on 10 kPa gel than the comparable adherent cells. Cells were highly deformed in the cytometry channel [Fig. S2(c)]. Similar differences (between adherent and nonadherent cells) were observed in cell area [Fig. S2(d)] and volume (Fig. S2), in cells seeded on 100 kPa gel substrates. The larger morphology attributable to PAX exposure also contributed to higher cell deformation within the channel [Fig. S2(f)].

We then examined how increasing substrate stiffness alone and in conjunction with local compression via seeding at increased density influences cells' collective mechanoadaptation to substrate stiffness. First, we measured the change from 24 to 72 h in bulk modulus of cells seeded on substrates of increasing stiffness, *i.e.*, proliferating from LD to HD over 72 h. Cells exhibited bulk modulus stiffening resulting in a closer match to the stiffness of their respective substrates, with a mean Modulus of 7.7 kPa on the 10 kPa substrate and 22.1 kPa on the 100 kPa substrate [Fig. 5(a)]. Finally, exposure of cells to local compression by seeding at HD resulted in greater mechanoadaptation as measured by relative changes intrinsic cell stiffness than exposure to PAX [Fig. 5(b)]. With PAX treatment, the mean bulk modulus of cells seeded at HD was higher than that of control cells, *i.e.*, 13 kPa on the 10 kPa substrate and 28.3 kPa on the 100 kPa substrate, a difference that is comparable to that of LD cells [Fig. 5(b)].

PAX-exposed stem cells adapt more readily to soft substrates via increasing actomyosin contractility

Despite the lower degree of actin alignment and its small difference after PAX treatment, the mean Young's Moduli of stem cells cultured on soft substrates were higher than those cultured on glass, i.e., almost matched the Young's Modulus of the gel. As stem cells show better capacity to adapt on softer substrates than on glass, with gels being more deformable or within stiffness ranges that cells can reciprocate with active pulling/tension, we then questioned the role of myosin II contractility in facilitating this adaptation. We probed for the expression of three myosin II isoforms that perform independent functions in maintaining cellular tension during adhesion.

We found that the expression of Myosin IIA and IIB increases with increasing substrate stiffness, whereas the expression of Myosin IIC decreases [Fig. 6(a)]. PAX treatment enhances the expression of the three Myosin II isoforms, i.e., Myosin IIA, IIB, and IIC. Notably, the increase in Myosin IIA expression upon PAX treatment is higher on glass than on softer gels [Fig. 6(b)]. In contrast, the increase in Myosin IIB and IIC expression is much larger on soft substrates than on glass [Figs. 6(c) and 6(d)].

We summarize the experimental results regarding Myosin II contractility on stem cell adaptation to soft substrates in Figs. 6(e) and 6(f). With relatively softer substrates, control cells exhibited more F-actin crosslinks and short actin fibers oriented in random directions. With PAX exposure, a majority of stress fibers align within the cells;

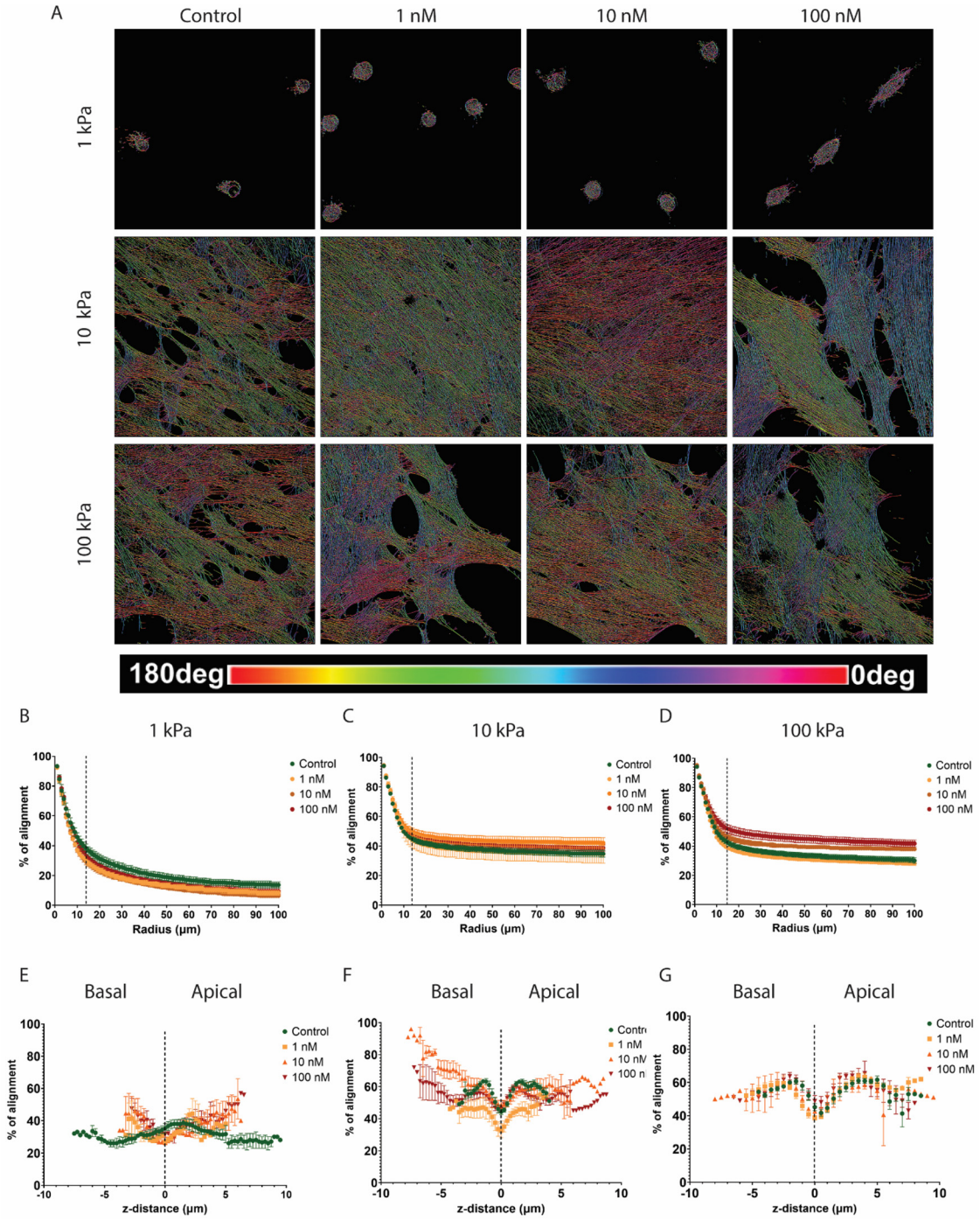

FIG. 3. Actin filament alignment serves as a major change in phenotype during stem cell adaptation to substrate stiffness and stabilization of microtubules with PAX. (a) NoBS of actin reveals how substrate stiffness modulates the PAX-induced actin ordering. After 72 h culture on (b) 1 and (c) 10 kPa gels, PAX-treated cells show a lower degree of actin alignment and a smaller difference between treated groups. (d) On 100 kPa gel, PAX-treated cells exhibit a higher degree of actin alignment than the control cells, although not as significant as those seeded on glass. The differences in apical and basal actin alignment on the softer gels, 1 kPa (e), 10 kPa (f), and 100 kPa (g), across the PAX exposed groups are less distinct than those on glass. Nuclear z-thickness is used to determine the mid-plane of the cell (marked as dotted line at 0 μm) and to define the apical (top) and basal (bottom) regions. Although a clear distinction between apical and basal region can be observed with increasing substrate stiffness, there is no difference in the apical-basal actin alignment between the control and PAX-treated cells on soft substrates.

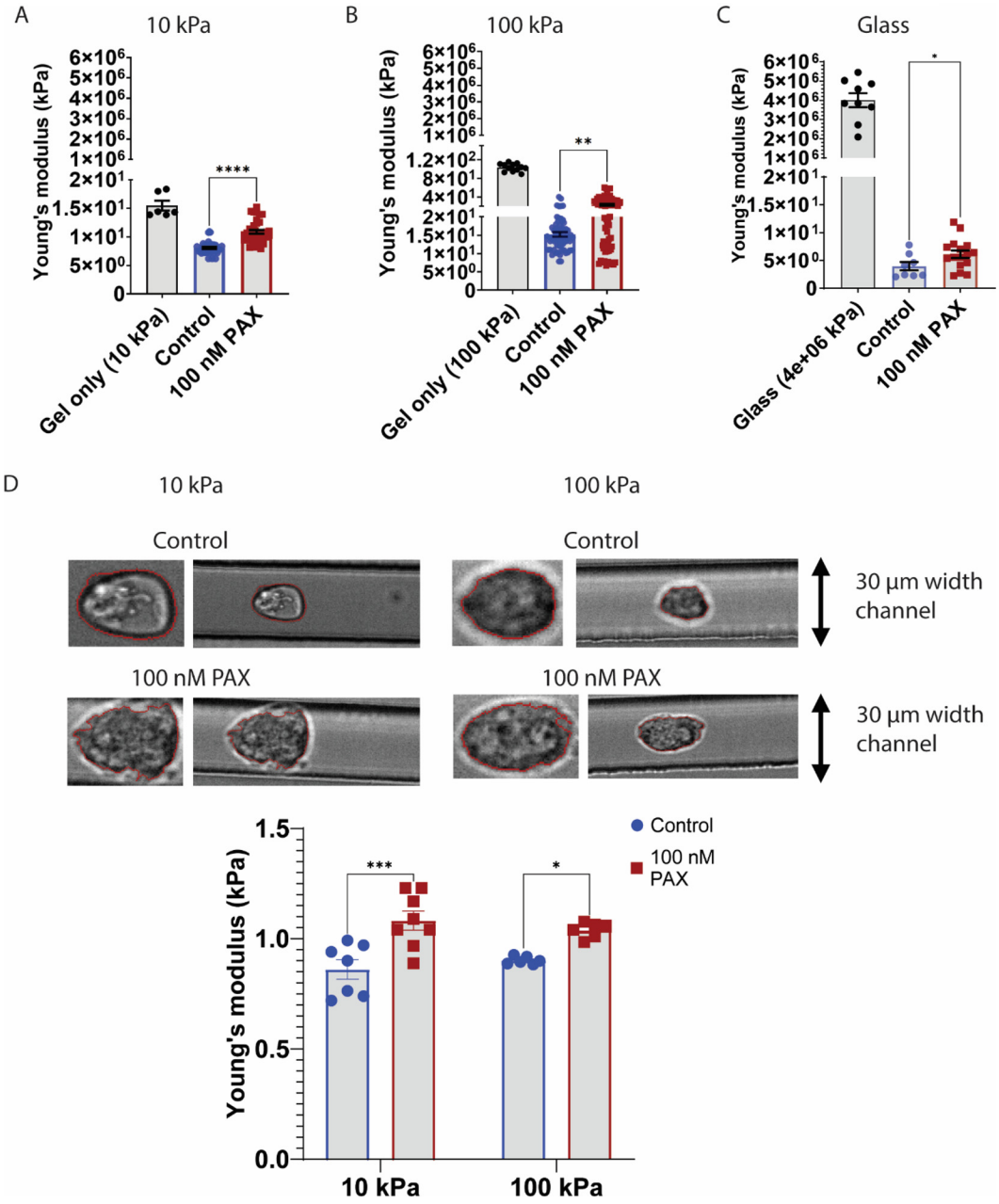

FIG. 4. Young's Moduli of cells cultured on substrates of increasing stiffness. Measurement of cell modulus via AFM revealed that on (a) 10 kPa and (b) 100 kPa hydrogels, PAX-exposed cells adapted more readily to match the stiffness of the gels than when cultured on glass (c). Data for each condition were acquired from measurement of 10–15 independent cells and presented as mean ± SEM. The differences in Young's Moduli between the control and PAX-treated cells were more significant on the gels than on glass. (d) The significant stiffening effect of PAX exposure to cells was maintained even when the cells were trypsinized, and the Young's Moduli of the same cells in suspension were measured via deformability cytometry after culture on 10 and 100 kPa gels and treated with PAX for 24 h.

however, a greater number of short actin protrusions in random orientations and actin crosslinks between the aligned stress fibers were also observed. Taken as a whole, this not only contributes to lower global actin alignment when quantified with NoBS but also accounts for the much larger difference in Young's Modulus and Myosin IIB expression between the control and PAX-exposed groups. In contrast, for cells seeded on glass substrates, PAX induces long and thick, highly aligned actin stress fibers, resulting in higher Young's Moduli and Myosin II B expression, although with less significant effects than for cells seeded on soft gels.

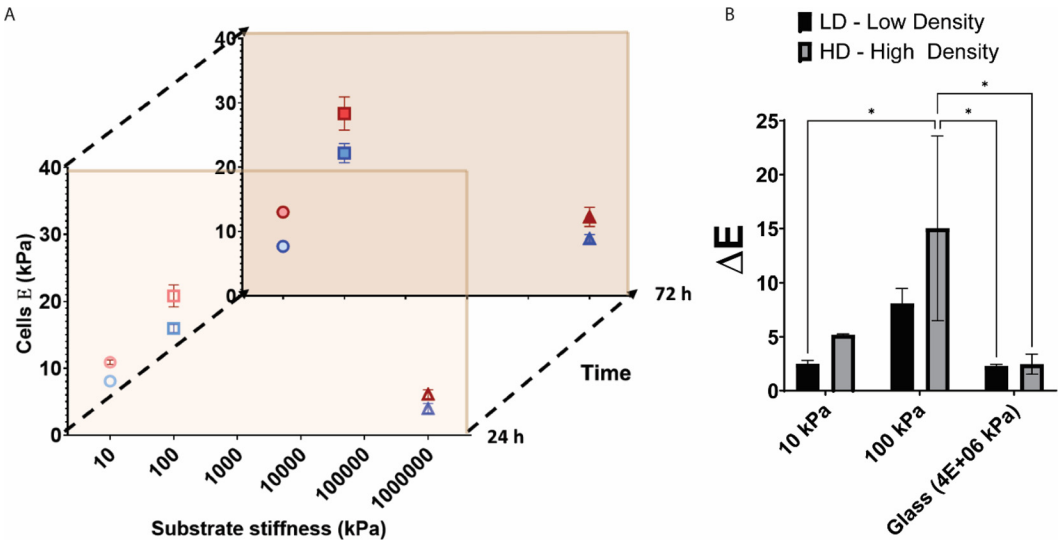

FIG. 5. Differences in cells' Young's Moduli when cultured on substrate with increasing stiffness, demonstrating their adaptation in mechanical properties, and effect of seeding at higher initial densities, imparting local compression to cells. (a) Spatiotemporal changes of Young's Moduli as they proliferated from low density (LD) at 24 h to high density (HD) at 72 h and adapted to the different substrate stiffness during PAX treatment. (a) is designed to serve as a summary figure for all the AFM measurements made on cells seeded at low density (24 h) and as they proliferated to target density (72 h) on substrates of increasing compliance. The data points are positioned to indicate time progression as cells adapt their mechanical properties to substrates. Empty (shape outlines) and color-filled data points (shape outlines) represent the respective 24 and 72 h timepoints. Data point shape ties the same experimental groups across time. (b) Changes in the Young's Moduli (ΔE) of PAX exposed cells when seeded at LD or HD on different hydrogel substrates. Asterisk represents significant differences at $^{*}p < 0.05$. Tukey's multiple correlation.

Testing statistical correlations between independent and dependent variables and an animation to integrate and interpret results

To test independent effects of increasing substrate compliance, exposure to PAX, seeding at increasing cell density and decoupling of the cell from its native environment (suspension), we analyzed the correlation matrix between all dependent variables measured in this study (pooled data), indicating the level of interaction between cytoskeletal adaptation and remodeling parameters (Table I). These dependent variables included cell volume, actin alignment as well as actin and microtubule concentration (volume within cell). We defined significance in context of the experimental model system where exposure to PAX is known to stabilize polymerized microtubules by decreasing depolymerization; as such, with the correlation significant at the 0.01 level (2-tailed), the 0.332 correlation coefficient between per cell microtubule concentration and PAX concentration can be considered to be strongly correlated. By defining a physiologically relevant, strong correlation in this way, other calculated correlation values can be considered relative to that known strong correlation. Positive and negative, significant correlation coefficients corroborate results observed in each of the experimental studies described earlier and discussed in detail later.

Finally, we integrate and summarize the experimental results graphically in an animation (Animation 1).

DISCUSSION AND CONCLUSION

The current study (Part II) probed mechanoadaptation of MSCs in response to controlled biophysical cues known to induce local compression (seeding at increased density) and tension (seeding on compliant substrates), akin to mechanical testing of the most basic living and adapting unit of life. We exogenously perturbed the intrinsic capacity of MSCs to adapt via exposure to specific concentrations of PAX, which inhibited microtubule depolymerization, as developed in Part I of the study (Part I). Yet, stem cell mechanoadaptation to substrates of increasing stiffness was more pronounced than adaptation to exogenous cytoskeletal (tubulin) depolymerization inhibitors. Increasing PAX concentration up to 100 nM increased cell stiffness and volume, with associated emergent anisotropic cytoskeletal architectures. Probing of myosin II expression demonstrated that the MSCs adapted more readily on compliant substrates by virtue of their actomyosin contractility, i.e., active mechanoadaptation.

While stabilization of microtubules leads to an increase in actin length and alignment, providing a means to efficiently distribute larger forces within the cells, the degree of actin alignment is predominantly regulated by substrate (local environment) rigidity sensing. On glass, cells exhibit a clear PAX concentration-dependent stress fiber (SF) alignment, where at 100 nM PAX, a majority of SFs align in predominant directions. On compliant gels, this concentration-dependent increase in SF alignment is abolished, and short, random F-actin cross-links are present along with aligned SFs, contributing to a lower alignment score. This is consistent with the reported regulation of fluid-like to solid-like actin behavior that depends mainly on substrate stiffness and not cell shape.[13] Furthermore, cells cultured on a circular shape pattern on a soft substrate possess high actin fluidity, though with increasing substrate stiffness, actin remodels into higher order with unidirectional alignment while maintaining cell circular shape. Regardless of shape, stiff substrates prompt actin nematic behavior to exert larger traction force on opposite sides of cell periphery.[13,14] However, without shape confinement, cells would spread and initiate

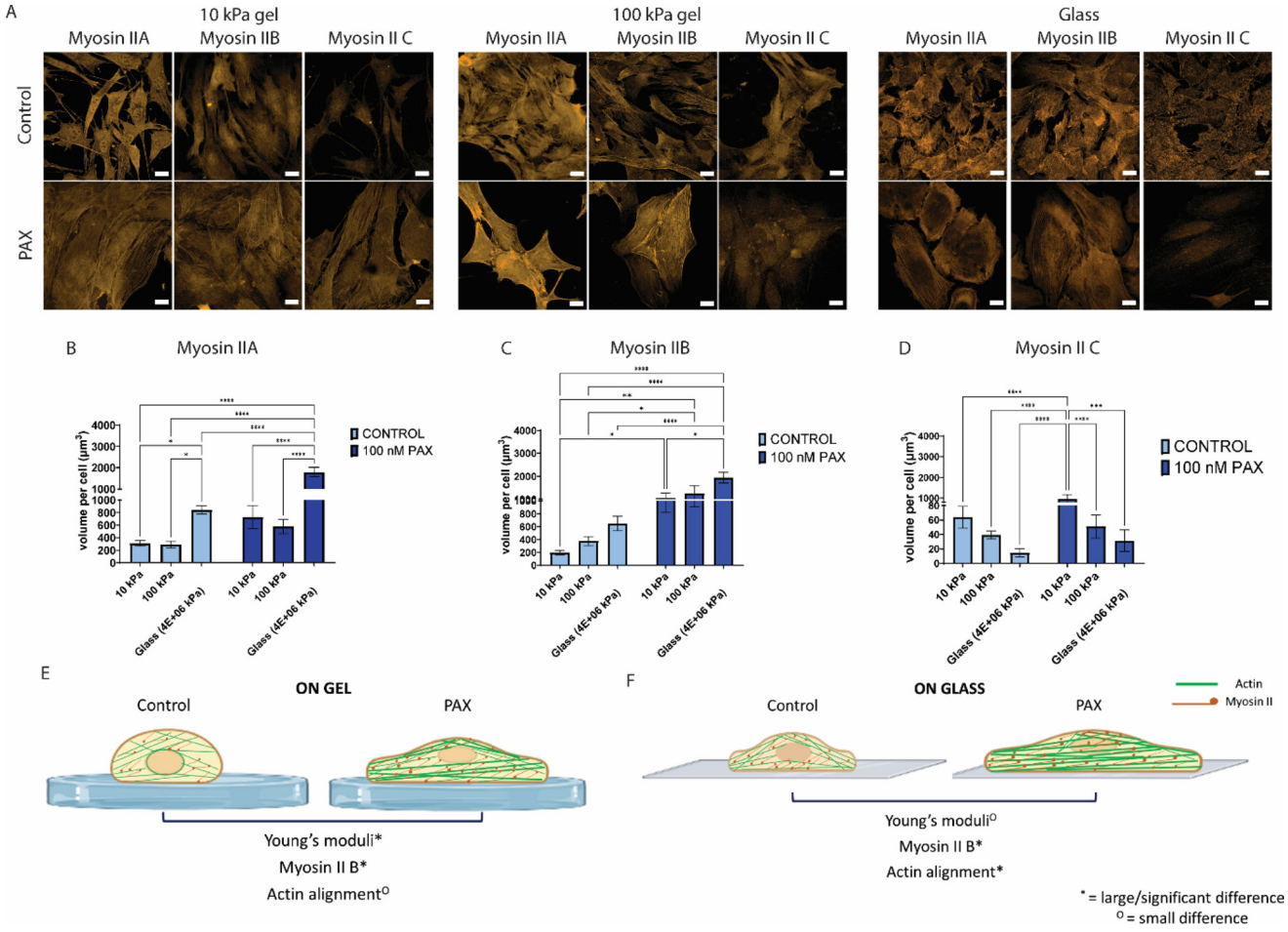

FIG. 6. Stem cells adapt more readily on compliant substrates by means of their actomyosin contractility. PAX exposed stem cells exhibit significantly larger mean Young's Moduli than those of control cells on compliant substrates, but not on glass, which corresponds with their significant increase in Myosin II expression (a), particularly Myosin II B. (b) Myosin II A expression as a function of substrate stiffness and PAX treatment. (c) Myosin II B expression shows significantly larger differences on softer substrates. (d) In contrast, Myosin II C expression decreases with increasing substrate stiffness but with larger difference with PAX treatment on softer substrates. Stem cell adaptation to substrate stiffness is by means of their actomyosin contractility that is more permissible on softer substrates (e) than on glass (f). Scale bar = 20 μm. Asterisks indicate significant differences at $^{*}p < 0.05$, $^{**}p < 0.01$, $^{***}p < 0.001$, and $^{****}p < 0.0001$ (Tukey's multiple correlation).

anisotropic focal adhesion points on the substrate, enabling a more effective force distribution.

In this study, SA/V, defining cell shape, increases with increasing PAX concentration in parallel with the increase in actin alignment on glass, whereas culture on gels seems to maintain SA/V across PAX concentration. This may be attributable to the fact that cells require a minimum area of spreading to survive.[15] Typical culture on glass or dishes provides unlimited adhesive substrate to the cells, and hence, when combined with PAX, treatment compromises cell shape stability or isometric tension (pre-stress), which are otherwise maintained by the cell–cell and cell–extracellular matrix (ECM) interaction within physiological tissue.[16]

The cytoskeleton within the cell represents a system that maintains shape stability through adjustment/adaptation of pre-stress, and the non-zero tensile stress of the actin filaments presents when no external forces are acting on the cell boundary.[17] Microtubules are known to balance a portion of this tensile stress, which serves as a means for cells to oppose changes in shape. However, when microtubule polymerization is disrupted (e.g., by colchicine), these stresses would shift to the substrate, resulting in an increase in traction force,[18] provided that the substrate is compliant. Hypothetically, when microtubules are stabilized with PAX, the stress would be instead borne by the cells causing actin SFs to grow linearly, unbranched, and thicker, which, in turn, would compromise cell shape as seen in the increasing SA/V. Particularly, when the substrate is within the compliant range that cells can readily deform, dramatic changes in the F-actin observed in this study must occur to achieve minimal energy stored within the structure (force balance) and providing a mechanism whereby PAX treated cells could match the stiffness of the gel substrate. Cytoskeleton dynamics allows the unpredictable fluctuations of traction forces at the cell–substrate interface as a means to maintain tensional homeostasis.[19] Over time, the cytoskeleton maintains this fluctuation within a

TABLE I. The correlation matrix showing the correlation coefficient between all independent variables (microtubule stabilization via PAX, seeding density, substrate stiffness) and outcome variables measured in this study (pooled data) and indicating the level of interaction between cytoskeletal adaptation or remodeling parameters: cell volume, actin alignment, and actin and microtubule concentration. Green cells indicate a positive correlation (see details later), red cells indicate a negative correlation, and gray cells indicate no correlation. Values indicate Pearson's correlation coefficient. In context of this experimental model system where exposure to PAX is known to stabilize polymerized microtubules by decreasing depolymerization, the 0.332 linear correlation coefficient between per cell microtubule concentration and PAX concentration can be considered as strongly correlated, and other correlation values can be considered relative to that known correlation.

	Correlations										
	PAX concentration	Substrate stiffness	Seeding density	Cell volume	Actin concentration	Microtubule concentration	Actin alignment	Young's modulus	MyoIIA concentration	MyoIIB concentration	MyoIIC concentration
PAX concentration		−0.144[a]	0.013	0.341[a]	0.328[a]	0.332[a]	0.287[a]	0.263[a]	0.342[a]	0.463[a]	0.348[a]
Substrate stiffness	−0.144[a]		0.215[a]	0.404[a]	0.174[a]	0.171[a]	−0.040	−0.371[a]	0.469[a]	0.257[a]	−0.152[b]
Seeding density	0.013	0.215[a]		0.285[a]	−0.184[a]	−0.111[b]	−0.190[b]	0.228[a]	.[c]	.[c]	.[c]
Cell volume	0.341[a]	0.404[a]	0.285[a]		0.244[a]	0.416[a]	−0.121	−0.039	0.404[a]	0.172[b]	0.196[a]
Actin concentration	0.328[a]	0.174[a]	−0.184[a]	0.244[a]		0.380[a]	0.235[a]	−0.116[b]	0.370[a]	0.240[a]	−0.161[b]
Microtubule concentration	0.332[a]	0.171[a]	−0.111[b]	0.416[a]	0.380[a]		0.301[a]	−0.113	0.366[a]	0.242[a]	−0.114
Actin alignment	0.287[a]	−0.040	−0.190[b]	−0.121	0.235[a]	0.301[a]		0.103	0.202	0.173	−0.058
Young's modulus	0.263[a]	−0.371[a]	0.228[a]	−0.039	−0.116[b]	−0.113	0.103		−0.119	−0.033	−0.007
MyoIIA concentration	0.342[a]	0.469[a]	.[c]	0.404[a]	0.370[a]	0.366[a]	0.202	−0.119		0.250[a]	0.053
MyoIIB concentration	0.463[a]	0.257[a]	.[c]	0.172[b]	0.240[a]	0.242[a]	0.173	−0.033	0.250[a]		0.115
MyoIIC concentration	0.348[a]	−0.152[b]	.[c]	0.196[a]	−0.161[b]	−0.114	−0.058	−0.007	0.053	0.115	

[a]Correlation is significant at the 0.01 level (2-tailed).
[b]Correlation is significant at the 0.05 level (2-tailed).
[c]Cannot be computed because at least one of the variables is constant.

small range that could be matched with the mean traction force exerted onto the substrate.[19]

Simultaneously, cells have the capacity to adapt to their surrounding mechanical properties and tune their internal stress to match the stiffness of their underlying substrates,[19,20] which seems to be permissible within a certain range of substrate stiffness. On substrates of 0.5–40 kPa, fibroblasts become stiffer as substrate stiffness increases before finally achieving a constant Young's Modulus on 20 kPa substrates and above.[12] In this study, C3H/101/2 exhibits a mean Young's Modulus of 3.3 kPa and about twice higher mean of Young's Modulus of 6.4 kPa, upon PAX treatment, when probed on glass. Interestingly, cells reach mean Young's moduli of 8.806 and 15.25 kPa when probed on compliant 10 and 100 kPa gel substrates, respectively. PAX treatment increases cells' Young's Moduli to closely match the moduli of the compliant substrate, i.e., 10.9 and 23.08 kPa on 10 and 100 kPa gels, respectively. With microtubule disruption (PAX exposure), the energy stored in the compliant substrate is calculated as the work done by traction to deform the substrate, which, in this case, translates to the larger Young's Moduli on compliant substrates than those on stiffer glass substrates.

Cell proliferation toward higher density represents the natural progression of cell growth and division, which influences how cells sense their local mechanical environment and dictate tissue morphogenesis.[21,22] When cells proliferate to higher density, the increase in cell bulk modulus upon PAX treatment was significantly larger on gel substrates than on glass. In the context of a multicellular construct, high density (HD) cells experience larger compression from the neighboring cells, which balances the cells' collective tensile forces. Particularly, tissues or multicellular constructs remodel extracellular matrix to achieve the balance of force exerted by the ECM on cells and forces generated by the cells themselves onto the ECM.[23] PAX treatment increases cell volume and microtubule pushing forces, thus elevating the compression between cells. When cells were cultured on gel substrates, the excess energy from that pushing forces could be distributed and stored within the actin, microtubule, and gel network, so that HD cells could readily achieve force balance—exhibiting stiffness that closely matches the gel substrates. HD cells proliferating to higher density are evidently more tensile on soft gels than on stiff gels.[24] On softer substrates, HD cells in multiple 3D layers sense rigidity by dynamically adjusting their adhesion and tuning the low or high interactions with the substrate, allowing them to be more or less tensile.[24]

While it is counterintuitive that cells exhibit reduced stress fiber alignment on softer substrates despite their higher Young's Moduli compared to stiff glass substrate, cells on compliant substrates exhibit more short actin structures with random orientation across the basal to apical regions and higher expression of Myosin II isoforms, indicative of contractility. In this study, we use exogenous PAX exposure to decipher the relationship between actin fiber rearrangements and cell stiffness adaptation, as a means to distribute stress efficiently, particularly for cells cultured on gel substrates. With exogenous microtubule stabilization via PAX exposure, increased concentrations of Myosin IIA, IIB, and IIC were consistently observed. This may be attributable to the increase in the F-actin length, thickness, and overall concentration per cell triggering compensatory mechanisms for cells to maintain contractility via higher levels of myosin binding on F-Actin. Interestingly, with increasing substrate stiffness, opposite trends were observed, i.e., Myosin IIC expression was observed to decrease. Compliant substrates allow cells to exert larger traction force by means of randomly oriented and shorter F-actin or via actin rearrangements and myosin contractility. In particular, the larger increase in Myosin IIB and IIC expression on soft gels compared to stiff glass demonstrates the activity of those isoforms as endogenous stress-generation-dependent vs (over) purely substrate-stiffness-dependent. Given the role of Myosin IIB in bearing larger loads (higher duty ratio) and in polarization of traction forces,[25] PAX-stabilized microtubules might require a higher increase in IIB and IIC in conjunction with the increase in actin crosslinks. In contrast, Myosin IIA, as the major Myosin II isoform,[25] increases its expression with increasing substrate stiffness and plays a critical role in generation of traction force and determination of cell polarity. Myosin IIA and IIB are reported to perform contrasting mechanical roles in cell spreading, whereby Myosin IIA retracts the lamellipodia extension mediated by Myosin IIB.[26] Hence, the difference in the increase in myosin isoforms' expression, cellular mechanical properties, and contractility observed in this study during the modulation of endogenous stress by PAX demonstrates the emergent adaptation to local environmental forces such as substrate rigidity and local compression. This emergent adaptation of F-actin and microtubules allows single cells and/or multicellular constructs to be more tensile and to tune their adhesion to a range of substrate stiffnesses. With respect to development and healing, such emergent adaptation is important for cells to establish the structure–function relationship of the tissues they build.[9]

Previous experience with primary murine embryonic cells derived from the mesoderm at E11.5,[28] human mesenchymal stem cells derived from periosteum, and commercially available stromal derived stem cells[29] demonstrates inherent advantages and limitations associated with each potential cell source. For donor cells, representation of a diverse population from a single or multiple cell donors is challenging even with very large sample sizes,[29] and neither hTERT cloning[30] nor iPS approaches[31] can completely overcome these inherent limitations. Ideally, we would aim to elucidate stem cell mechanoadaptation in live cells *in situ*, during embryonic development as it unfolds.[2] For the purpose of the current set of experiments, the C3H/10T1/2 cell line was chosen as a model embryonic murine mesenchymal stem cell line, to maximize comparison and build upon a knowledge base from previous published studies.[6,32–35] The mechanical and exogenous biochemical cues to which the cells were exposed include only a subset of the range of cues that cells experience *in situ*. The experimental approach lends itself to expansion, to include, e.g., a range of extracellular matrix proteins and/or presentation of cell-matrix adhesion molecules,[36] for probing of further specific effects on mechanoadaptation.

We fully expect to observe fundamental differences in cells derived from different species, reflecting the unique multi-length and multi-timescale mechanoadaptation capacities of those respective species.[2] It will be important and exciting to further characterize mechanoadaptation of stem cells derived from other sources, ideally including primary cells derived from human sources or *in situ* probing of mechanoadaptation in nonhuman embryos and in healing tissues of adult organisms, where healing putatively recapitulates developmental processes.[2] Such future studies would enable characterization of mechanoadaptation in response to a full range of realistic mechanical cues intrinsic to development *in utero* and putative recapitulation of developmental processes in postnatal life.

In the context of previously published work examining effects of substrate compliance,[37] cell seeding density and mode of achieving density,[32,34] and perturbing stem cells' mechanoadaptation capacity using exogenous means,[38,39] the current study combines these previous approaches to probe stem cell mechanoadaptation to stresses emulating those during development. Specifically, by exposing cells to local compression from increasing seeding density and local tension from compliant substrates, we probed the capacity of native and microtubule-stabilized cells to balance forces at cell boundaries via opposing shape changes and cytoskeletal reorganization (Animation 1, Table I). We also revealed how the interactions between independent variables (environmental cues) including tubulin stabilization (inhibiting tubulin depolymerization with PAX), increasing seeding densities (local compression), and substrate stiffness (local tension) influence the degree of F-actin and microtubule spatial distribution and reorganization as well as cell stiffness. By elucidating the cells' emergent adaptation to these local environmental cues, we demonstrate experimentally the hypothesized capacity of cells and the cytoskeleton to achieve tensional homeostasis in response to perturbation of cytoskeletal dynamics as well as changing mechanical and biophysical environmental cues intrinsic to tissue development in health and disease.

METHODS

Cell culture and Paclitaxel treatment

The C3H/10T1/2 murine embryonic stem cell line (CCL-226) was used as a model for primary embryonic mesenchymal stem cells and cultured in basal eagle medium (BME) with 1% penicillin-streptomycin, 1% L-glutamate, and 10% fetal bovine serum (FBS), per previously published protocols.[6,40] Cells were expanded and passaged to less than P15. For imaging, cells were seeded in glass-bottomed 24 well plates or 35 mm dishes coated with gel substrates of defined compliance (respective stiffness). For inducing local compression through seeding at increasing density,[27,40,41] cells were seeded at 5000 cells/cm^2 for low density (LD), 15 000 cells/cm^2 for high density (HD), and 45 000 cells/cm^2 for very high density (VHD).

Exogenous PAX exposure was carried out on the day following seeding. PAX solution was prepared from the stock of 5 mg/ml in Dimethyl Sulfoxide (DMSO) (5855 μM) in culture medium in a defined concentration range (1–100 nM). Medium was removed from the well plates, and PAX solution was added to the wells. Control cells were treated with medium containing only DMSO. Cells were incubated until used for assays or imaging at determined time points (24, 48, and 72 h). Throughout the study, outcome measures for cells exposed to microtubule stabilizing agent (PAX) were recorded at 24, 48, and 72 h. In consideration of C3H/10T1/2 doubling time, 72 h culture was needed for cells seeded at 5000 cells/cm^2 to achieve confluency, similar to achieving high density.

Polyacrylamide gel synthesis

Polyacrylamide gels, of 1, 10, and 100 kPa stiffness, were prepared as per our previous protocol.[42,43] Coverslips (18 mm) were first treated with 0.5% 3-aminopropyltrimethoxysilane solution and then with 0.5% glutaraldehyde solution. Glass slides were made hydrophobic by treatment with RainX. A mixture of polyacrylamide was prepared by varying the ratio of acrylamide and bisacrylamide monomers to achieve the desired stiffness. One mL of the polyacrylamide–acrylamide–bisacrylamide mixture was combined with 10 μl of 10% ammonium persulfate and 0.1 μl tetraethylmethylenediamine (TEMED). 20 μl of the resulting mixture was pipetted onto the treated coverslips, after which the coverslips with gel were immediately turned upside down, facing the treated glass slide. The gels were left to polymerize for 10 min. The gels were then treated with 55% aqueous hydrazine hydrate for 2 h, followed by washing with de-ionized water and glacial acetic acid for 1 h each. Fibronectin was added into 3.5 mg/ml sodium periodate solution and was incubated for 30 min to oxidize the protein. 200 μl of the protein solution was pooled onto a polydimethylsiloxane (PDMS) stamp and incubated for 1 h. The stamps were air dried and then placed face down on to the PA gel surface. The stamp was lifted carefully, resulting in a gel with fibronectin surface coating, which was washed with de-ionized water and PBS and then sterilized under UV before being used as cell culture substrate.

Cell and cytoskeleton imaging and analysis

Cells were labeled with Calcein AM and Hoechst stain for imaging of cell and nucleus structures. Actin was labeled using Actin Green^{TM} (LifeTech) with fluorophores that excite at 488 nm. Microtubule cytoskeleton as well as the three myosin II isoforms, Myo IIA, B, and C, were labeled using antibodies-based incubation [Anti tubulin antibody (LifeTech Cat. No. A11126, 1:300 dilution), anti-Myosin IIA and anti-Myosin IIB (BioLegend, Poly19098 and Poly19099, 1:250 dilution), and anti-Myosin IIC antibody (Cell signaling, Cat. No. 3405, 1:300)], as described in the preceding study (Part I). The analysis of cell shape and volume as well as cytoskeleton spatial distribution and actin fiber remodeling were quantified using custom MATLAB and Image J macro scripts, as described in the preceding study (Part I).

Atomic force microscopy (AFM)

Cells were seeded onto fibronectin coated polyacrylamide gels of various compliance at low density (LD), i.e., 5000 cells/cm^2, and high density (HD), i.e., 15 000 cells/cm^2, and treated with PAX for 24–72 h. Medium was replaced with serum free and phenol red free standard medium. Cells were taken for AFM measurement and analysis of cell Young's Modulus following the protocols described in the preceding study (Part I). AFM measurement of cells seeded on gel substrates (Fig. 5) was carried out at 24 and 72 h to correspond to cells at low- and high-density states, respectively.

Deformability cytometry

Cells were seeded onto polyacrylamide gels on 25 mm coverslips in 6 well plates. Cells were treated the next day with 100 nM PAX or DMSO for control. After 48 h, the cells were harvested and centrifuged, and the pellet was washed in PBS and resuspended in Cell Carrier buffer (Zellmechanik) for deformability cytometry analysis, as described in the preceding study (Part I).

Statistical analysis

Statistical analysis of experimental data was performed using Graphpad prism (La Jolla, CA) and SPSS (IBM). Significant differences in cell volume, stiffness, actin, and microtubule concentration across PAX concentration, substrate stiffness, and seeding densities were analyzed with two-way ANOVA and the Tukey's multiple comparison

test. A linear mixed model test was performed using the SPSS to investigate the effects of interacting variables on cells' Young's Modulus; this included a test of three-way interaction between independent variables: cell seeding density, substrate stiffness, and PAX concentration, where data from each condition for each cell and repeat were pooled (Table S1). Bivariate Pearson's correlation analysis between the dependent variables such as cell volume, actin and microtubule concentration, actin alignment, and Young's Modulus was performed to test how correlated their measures were from the three independent variables. The computed Pearson's correlation coefficient with two-tailed test of significance was used to define the negative, positive correlation, or no correlation (Table I). As not all possible combinations of variables were tested in this study, two-way ANOVA was also performed to test the interaction between two independent variables in modulating cell volume, actin and microtubule concentration, and actin alignment (Table S2).

SUPPLEMENTARY MATERIAL

See the supplementary material for further details of intergroup statistical comparisons.

ACKNOWLEDGMENTS

The authors would like to acknowledge the Katharina Gaus Light Microscopy Facility (KGLMF) and their staff for the continuous support in imaging resources and assistance in image processing and analysis, as well as Professor Peter Gunning for discussions and suggestions regarding the myosin isoform experimental design. The authors would like to thank Dr. Michael Carnell for developing the NoBS algorithm for the analysis of F-actin stress fibers alignment; Dr. Elvis Pandzic for assisting and training V.P. in custom-built MATLAB scripts for the analysis of cell shape and volume; Dr. Celine Heu for assistance with the AFM; Dr. Chantal Kopecky for assistance in deformability cytometry; and Dr. Mark Donoghoe from the Kirby Institute for statistical expertise. V.P. would like to acknowledge the Scientia Ph.D. Scholarship scheme from UNSW for support throughout her doctoral research studies. This work has been supported in part by grants from the National Health and Medical Research Council (M. L.K.T. and K.A.K.), the National Institutes of Health (K.A.K.), and the Paul Trainor Family Chair Endowment (M.L.K.T.).

AUTHOR DECLARATIONS

Conflict of Interest

M.L.K.T. has co-founded startup companies to commercialize the intellectual property she and her collaborators have developed and patent protected over the past decades. The topic of the current manuscript is fundamental in nature and not directly related to M.L.K.T.'s innovation, translation and commercialization projects.

Ethics Approval

Ethics approval is not required.

Author Contributions

Vina D. L. Putra: Conceptualization (equal); Data curation (equal); Formal analysis (lead); Funding acquisition (supporting); Investigation (lead); Methodology (equal); Project administration (equal); Software (supporting); Validation (lead); Visualization (lead); Writing – original draft (lead); Writing – review & editing (equal). **Kristopher A. Kilian:** Conceptualization (equal); Data curation (supporting); Formal analysis (supporting); Funding acquisition (equal); Investigation (equal); Methodology (equal); Project administration (equal); Resources (equal); Software (supporting); Supervision (equal); Validation (supporting); Visualization (supporting); Writing – original draft (supporting); Writing – review & editing (supporting). **Melissa L. Knothe Tate:** Conceptualization (equal); Data curation (equal); Formal analysis (equal); Funding acquisition (equal); Investigation (equal); Methodology (equal); Project administration (equal); Resources (equal); Software (equal); Supervision (equal); Validation (equal); Visualization (equal); Writing – original draft (equal); Writing – review & editing (lead).

DATA AVAILABILITY

The data that support the findings of this study are available from the corresponding author upon reasonable request.

REFERENCES

[1]K. H. Vining and D. J. Mooney, "Mechanical forces direct stem cell behaviour in development and regeneration," Nat. Rev. Mol. Cell Biol. **18**(12), 728–742 (2017).
[2]M. L. Knothe Tate, P. W. Gunning, and V. Sansalone, "Emergence of form from function—Mechanical engineering approaches to probe the role of stem cell mechanoadaptation in sealing cell fate," Bioarchitecture **6**, 85 (2016).
[3]M. L. Knothe Tate, T. D. Falls, S. H. McBride, R. Atit, and U. R. Knothe, "Mechanical modulation of osteochondroprogenitor cell fate," Int. J. Biochem. Cell Biol. **40**(12), 2720–2738 (2008).
[4]E. Hannezo and C.-P. Heisenberg, "Mechanochemical feedback loops in development and disease," Cell **178**(1), 12–25 (2019).
[5]S. R. Moore, G. M. Saidel, U. Knothe, and M. L. Knothe Tate "Mechanistic, Mathematical Model to Predict the Dynamics of Tissue Genesis in Bone Defects via Mechanical Feedback and Mediation of Biochemical Factors," PLoS Comp Biol **10**, e1003604 (2011).
[6]H. Chang and M. L. Knothe Tate, "Structure - Function relationships in the stem cell's mechanical world B: Emergent anisotropy of the cytoskeleton correlates to volume and shape changing stress exposure," Mol. Cell. Biomech. **8**(4), 297–318 (2011).
[7]S. H. McBride, S. Dolejs, S Brianza, U. Knothe, and M. L Knothe Tate, "Net Change in Periosteal Strain During Stance Shift Loading After Surgery Correlates to Rapid De Novo Bone Generation in Critically Sized Defects," Ann. Biomed. Eng. **39**(5), 1570–1581 (2011).
[8]N. Y. C. Yu, C. A. O'Brien, I. Slapetova, R. M. Whan, and M. L. Knothe Tate, "Live Tiss Imaging to Elucidate Mechanical Modulation of Stem Cell Niche Quiescence," Stem Cells Transl Med **6**(1), 285–292 (2017).
[9]J. Zimmerman and M. L. Knothe Tate, "Structure- Function relationships in the stem cell's mechanical world A: Seeding protocols as a means to control shape and fate of live stem cells," Mol. Cell. Biomech **8**(4), 275–296 (2011).
[10]S. B. Khatau *et al.*, "A perinuclear actin cap regulates nuclear shape," Proc. Natl. Acad. Sci. USA **106**, 19017 (2009).
[11]V. D. L. Putra, K. A. Kilian, and M. L. Knothe Tate, "Stem cell mechanoadaptation. I. Effect of microtubule stabilization and vol changing stresses on cytoskeletal remodeling," APL Bioeng. **8**(4), 016102 (2024).
[12]J. Solon, I. Levental, K. Sengupta, P. C. Georges, and P. A. Janmey, "Fibroblast adaptation and stiffness matching to soft elastic substrates," Biophys. J. **93**(12), 4453–4461 (2007).
[13]M. Gupta *et al.*, "Cell shape and substrate stiffness drive actin-based cell polarity," Phys. Rev. E **99**(1–1), 12412 (2019).
[14]M. Gupta *et al.*, "Adaptive rheology and ordering of cell cytoskeleton govern matrix rigidity sensing," Nat. Commun. **6**, 7525 (2015).

[15]C. S. Chen, M. Mrksich, S. Huang, G. M. Whitesides, and D. E. Ingber, "Geometric control of cell life and death," Science **276**(5317), 1425–1428 (1997).
[16]T. Manuel *et al.*, "Anisotropy of cell adhesive microenvironment governs cell internal organization and orientation of polarity," Proc. Nat. Acad. Sci. **103**(52), 19771–19776 (2006).
[17]N. Wang *et al.*, "Cell prestress. I. Stiffness and prestress are closely associated in adherent contractile cells," Am. J. Physiology-Cell Physiology **282**(3), C606–C616 (2002).
[18]D. Stamenović, S. M. Mijailovich, I. M. Tolić-Nørrelykke, J. Chen, and N. Wang, "Cell prestress. II. Contribution of microtubules," Am. J. Physiol. -Cell Physiol. **282**(3), C617–C624 (2002).
[19]D. Stamenović and M. L. Smith, "Tensional homeostasis at different length scales," Soft Matter **16**(30), 6946–6963 (2020).
[20]D. Stamenović and N. Wang, "Stress transmission within the cell," Compr. Physiol. **1**(1), 499–524 (2011).
[21]T. Lecuit and P.-F. Lenne, "Cell surface mechanics and the control of cell shape, tissue patterns and morphogenesis," Nat. Rev. Mol. Cell Biol. **8**(8), 633–644 (2007).
[22]C. Cadart, L. Venkova, P. Recho, M. C. Lagomarsino, and M. Piel, "The physics of cell-size regulation across timescales," Nat. Phys. **15**(10), 993–1004 (2019).
[23]C. C. DuFort, M. J. Paszek, and V. M. Weaver, "Balancing forces: Architectural control of mechanotransduction," Nat. Rev. Mol. Cell Biol. **12**(5), 308–319 (2011).
[24]S. Sonam *et al.*, "Mechanical stress driven by rigidity sensing governs epithelial stability," Nat. Phys. **19**(1), 132–141 (2023).
[25]Y. Peng *et al.*, "Non-muscle myosin II isoforms orchestrate substrate stiffness sensing to promote cancer cell contractility and migration," Cancer Lett. **524**, 245–258 (2022).
[26]V. Betapudi, "Myosin II motor proteins with different functions determine the fate of lamellipodia extension during cell spreading," PLoS One **5**(1), e8560 (2010).
[27]J. A. Zimmermann and M. L. Knothe Tate, "Structure - Function relationships in the stem cell's mechanical world A: Seeding protocols as a means to control shape and fate of live stem cells," Mol. Cell. Biomech. **8**(4), 275–296 (2011).
[28]M. Knothe Tate, T. Falls, S. Mishra, and R. Atit, "Engineering an ecosystem: Taking cues from nature's paradigm to build tissue in the lab and the body," in *New Perspectives in Mathematical Biology* (Fields Institute for Mathematics in Biology, 2010), Vol. 57, pp. 113–132.
[29]H. Chang, D. Docheva, U. R. Knothe, and M. L. Knothe Tate, "Arthritic periosteal tissue from joint replacement surgery: A novel, autologous source of stem cells," Stem Cells Transl. Med. **3**(3), 308–317 (2014).
[30]W. Böcker *et al.*, "Introducing a single-cell-derived human mesenchymal stem cell line expressing hTERT after lentiviral gene transfer," J. Cell. Mol. Med. **12**(4), 1347–1359 (2008).
[31]J. Cerneckis, H. Cai, and Y. Shi, "Induced pluripotent stem cells (iPSCs): Molecular mechanisms of induction and applications," Signal Transduction Targeted Ther. **9**(1), 112 (2024).
[32]S. H. McBride and M. L. Knothe Tate, "Modulation of stem cell shape and fate A: The role of density and seeding protocol on nucleus shape and gene expression," Tissue Eng., Part A **14**(9), 1561–1572 (2008).
[33]S. H. McBride, T. Falls, and M. L. Knothe Tate, "Modulation of stem cell shape and fate B: Mechanical modulation of cell shape and gene expression," Tissue Eng., Part A **14**(9), 1573–1580 (2008).
[34]J. A. Zimmermann and M. L. Knothe Tate, "Structure - Function relationships in the stem cell's mechanical world A: Seeding protocols as a means to control shape and fate of live stem cells," Mol. Cell. Biomech. **8**(4), 275–296 (2011).
[35]M. J. Song, S. M. Brady-Kalnay, S. H. McBride, P. Phillips-Mason, D. Dean, and M. L. K. Tate, "Mapping the mechanome of live stem cells using a novel method to measure local strain fields in situ at the fluid-cell interface," PLoS One **7**, e43601 (2012).
[36]S. F. Evans, D. Docheva, A. Bernecker, C. Colnot, R. P. Richter, and M. L. Knothe Tate, "Solid-supported lipid bilayers to drive stem cell fate and tissue architecture using periosteum derived progenitor cells," Biomaterials **34**, 1878 (2013).
[37]J. Solon, I. Levental, K. Sengupta, P. C. Georges, and P. A. Janmey, "Fibroblast adaptation and stiffness matching to soft elastic substrates," Biophys. J. **93**, 4453 (2007).
[38]F. Münz *et al.*, "Human mesenchymal stem cells lose their functional properties after paclitaxel treatment," Sci. Rep. **8**, 312 (2018).
[39]N. R. M. Beijer *et al.*, "Dynamic adaptation of mesenchymal stem cell physiology upon exposure to surface micropatterns," Sci. Rep. **9**, 9099 (2019).
[40]S. H. McBride and M. L. Knothe Tate, "Modulation of stem cell shape and fate A: The role of density and seeding protocol on nucleus shape and gene expression," Tissue Eng., Part A **14**(9), 1561–1572 (2008).
[41]M. J. Song, D. Dean, and M. L. Knothe Tate, "In situ spatiotemporal mapping of flow fields around seeded stem cells at the subcellular length scale," PLoS One **5**(9), e12796 (2010).
[42]J. Lee, A. A. Abdeen, Y. Li, S. Goonetilleke, and K. A. Kilian, "Gradient and dynamic hydrogel materials to probe dynamics in cancer stem cell phenotypes," ACS Appl. Bio Mater. **4**, 711 (2021).
[43]J. Lee, A. A. Abdeen, X. Tang, T. A. Saif, and K. A. Kilian, "Geometric guidance of integrin mediated traction stress during stem cell differentiation," Biomaterials **69**, 174–183 (2015).